Characterization of Stereochemistry and Molecular Conformation Using Solid-State NMR Tensors

James K. Harper, Anna E. Mulgrew, Jia Yao Li,† Dewey H. Barich, Gary A. Strobel,† and David M. Grant*

Contribution from the Department of Chemistry, University of Utah, Salt Lake City, Utah 84112

Received April 19, 2001. Revised Manuscript Received June 14, 2001

Abstract: A solid-state NMR technique is described for establishing stereochemistry using the natural product terrein as a model compound. This method involves comparison of experimental ^{13}C tensor principal values with ab initio computed values for all possible computer-generated stereoisomers. In terrein the relative stereochemistry is confirmed by NMR to be 2*R**,3*S** with high statistical probability (>99.5%). The proposed approach also simultaneously verifies the molecular conformation of the two hydroxy groups in terrein established by X-ray data. It is sufficient to use only shift tensor values at carbons 2 and 3, the stereocenters, to characterize both the stereochemistry and molecular conformations. The solid-state NMR method appears to be especially useful for determining relative stereochemistry of compounds or their derivatives that are difficult to crystallize.

Introduction

Determination of stereochemistry is an important step in the characterization of new materials, both of synthetic and natural origin. Such determinations are usually performed using X-ray diffraction or solution NMR. However, many materials fail to form crystals suitable for X-ray analysis or lack suitably positioned hydrogen nuclei, required for liquid NMR determinations. In such cases chemical shift tensor[1] values, provided by solid-state NMR, have the potential to identify the relevant stereochemistry. The chemical shift tensor, consisting of three principal shift values per nucleus, also provides valuable information for investigating simultaneously the molecular conformations.

Chemical shift tensor values have several potential advantages over the isotropic shift (i.e., the average of the principal values) commonly observed in liquids. Unlike the isotropic shift, the principal values are not averages and reflect strongly the local geometry. In addition, the orientations of the principal shift values have characteristic directions in a given molecular moiety. For example, the lowest-frequency (most-shielded) component (δ_{33}) in methyl groups lies generally along the $X-CH_3$ bond.[2] This directional property provides for a more direct correlation between tensor principal values and structure than found for isotropic shifts. Until the past few years, the experimental measurement of principal values has been difficult for relatively large molecules. Fortunately, new solid-state NMR techniques (e.g., FIREMAT or PASS)[3] now exist for measuring tensor principal values of all nuclei in natural abundance microcrystalline solids. These experiments take only a few hours in many cases. Using these techniques, samples containing up to 94 ^{13}C nuclei have been analyzed at natural abundance.[4]

Availability of experimental principal values has facilitated investigation of the correlation of molecular structure to shift tensor values. Such studies have demonstrated that tensor principal values are capable of accurately differentiating sheet and helical geometries in peptides[5] and characterizing molecular conformation in hydrocarbons and peptides.[6] Hydrogen-bonding distances have also proven to be correlated to ^{15}N and ^{13}C tensor components in peptides.[7] In addition, principal shift values have been found to reflect steric interactions in proximate methyl groups and in aromatic compounds.[2c,8] The variety of molecular phenomena to which tensors are sensitive suggests that principal values may provide sufficient information to establish stereochemistry. Herein, we investigate the sensitivity of ^{13}C tensor principal values to stereochemical differences in the natural product, terrein.

Experimental Section

Terrein was obtained by extraction of a culture solution of the fungus *Pestilotiopsis microspora*. Solutions were prepared by inoculating 16 L of M1D culture media[9] with *P. microspora* and incubating for 21 days at 23 °C. Solutions were then filtered through cheesecloth and

† Department of Plant Sciences, Montana State University, Bozeman, MT 59717.

(1) Grant, D. M. In *Encyclopedia of NMR*; Grant, D. M., Harris, R. K., Eds.; Wiley: Chichester, 1996; Vol. 2, pp 1298−1321.

(2) (a) Robyr, R.; Meier, B. H.; Fischer, P.; Ernst, R. R. *J. Am. Chem. Soc.* **1994**, *116*, 5315. (b) Soderquist, A.; Facelli, J. C.; Horton, W. J.; Grant, D. M. *J. Am. Chem. Soc.* **1995**, *117*, 8441. (c) Harper, J. K.; McGeorge, G.; Grant, D. M. *J. Am. Chem. Soc.* **1999**, *121*, 6488.

(3) (a) Alderman, D. W.; McGeorge, G.; Hu, J. Z.; Pugmire, R. J.; Grant, D. M. *Mol. Phys.* **1998**, *95*, 1113. (b) Orendt, A. M.; In *Encyclopedia of NMR*; Grant, D. M., Harris, R. K. Eds.; Wiley: Chichester, 1996; Vol. 2, pp 1282−1297. (c) Antzutkin, O. N.; Shekar, S. C.; Levitt, M. H. *J. Magn. Reson., Ser. A* **1995**, *115*, 7.

(4) Harper, J. K.; Barich D. H.; Grant, D. M. Manuscript in preparation.

(5) Havlin, R. H.; Le, H.; Laws, D. D.; de Dios, A. C.; Oldfield, E. *J. Am. Chem. Soc.* **1997**, *119*, 11951.

(6) (a) Harper, J. K.; Grant, D. M. *J. Am. Chem. Soc.* **2000**, *122*, 3708. (b) Wang, W.; Phung, C. G.; Alderman, D. W.; Pugmire, R. J.; Grant, D. M. *J. Am. Chem. Soc.* **1995**, *117*, 11984. (c) Heller, J.; Laws, D. D.; Tomaselli, M.; King, D. S.; Wemmer, D. E.; Pines, A.; Havlin, R. H.; Oldfield, E. *J. Am. Chem. Soc.* **1997**, *119*, 7827,

(7) (a) Gu, Z.; Zambrano, R.; McDermott, A. E. *J. Am. Chem. Soc.* **1994**, *116*, 6368. (b) Wei, Y.; de Dios, A. C.; McDermott, A. E. *J. Am. Chem. Soc.* **1999**, *121*, 10389. (c) Gu, Z.; McDermott, A. E. *J. Am. Chem. Soc.* **1993**, *115*, 4282.

(8) Facelli, J. C.; Orendt, A. M.; Jiang, Y. J.; Pugmire, R. J.; Grant, D. M. *J. Phys. Chem.* **1996**, *100*, 8268.

(9) Pinkerton, R.; Strobel, G. *Proc. Natl. Acad. Sci. U.S.A.* **1976**, *73*, 4007.

10.1021/ja010997l CCC: $20.00
Published on Web 09/15/2001

extracted three times with equal volumes of ethyl acetate. Ethyl acetate was removed by rotary evaporation, and the remaining solid was dissolved in 3:1 $CHCl_3/CH_3OH$ v/v and then applied to a silica gel column. Elution was performed using 20:1 $CHCl_3/CH_3OH$ v/v, and fractions were analyzed by TLC (silica, 8:1 $CHCl_3$/MeOH v/v, R_f = 0.51). All fractions containing terrein were pooled and dried by rotary evaporation. Further purification was achieved by passing through a second silica column using ethyl acetate/pentane (4:1 v/v). Fractions containing terrein were combined and rotary evaporated to dryness. Terrein was prepared for solid-state NMR by dissolving a 289 mg sample in methanol and allowing a crystalline solid to form by slow evaporation. Preparation by slow evaporation matches that reported in the X-ray analysis and ensures a sample directly comparable to the X-ray structure.[10] The resulting terrein consisted of reasonably large crystals that were ground to a powder for solid-state NMR analysis.

A 1D ^{13}C isotropic spectrum of terrein was obtained on a Chemagnetics CMX200 NMR using a 7.5 mm PENCIL probe and the TOSS pulse sequence.[11] The spectrum was acquired with a spectral width of 7.5 kHz, an operating frequency of 50.307995 MHz, and a decoupling frequency of 200.0448 MHz. TPPM ^1H decoupling[12] was used with an 8.2 μs 180° pulse and a phase angle difference of 18° between adjacent pulse segments. Other parameters include ^1H and ^{13}C 90° pulses of 4.1 and 4.05 μs, respectively, a spinning speed of 4000 Hz, a pulse delay of 45 s, a digital resolution of 4.9 Hz per point and a cross-polarization time of 2.5 ms. Ninety-six scans were collected, and the spectrum was referenced to the high-frequency peak of adamantane at 38.56 ppm.

FIREMAT analysis of terrein was performed under conditions similar to those for the TOSS spectrum, except that analysis was performed at a spinning speed of 468 Hz and all tensor principal values were extracted using previously described procedures and software.[3a,13] Evolution and acquisition spectral widths of 7.488 and 44.928 kHz, respectively, were used together with 16 evolution increments of 96 transients each and a 45 s pulse delay. A digital resolution of 11.7 Hz per point was realized in the acquisition dimension. An evolution dimension digital resolution of 11.7 Hz per point was obtained after the data replication and rearrangement required in the FIREMAT analysis.[3a]

Gauge invariant[14] tensor shielding values were computed with Gaussian 98[15] on IBM SP computers using parallel processing techniques. Calculated shieldings were converted to shifts using respective slope and intercept values of 1.006 and 194.933 for sp^2 carbons and 1.031 and 190.325 for sp^3 carbons. Such values have previously been found to give accurate shifts for large datasets of related natural products.[2c,16] Accurate conversion of shieldings to shifts in terrein was verified by calculating shift values for the X-ray structure and evaluating differences relative to the experimental values. An accurate conversion creates roughly equal numbers of overestimates and underestimates; thus, the summed differences are approximately zero. For terrein, the summed difference for all 24 principal values was 2.4 ppm validating the conversion process described. All geometries were optimized using

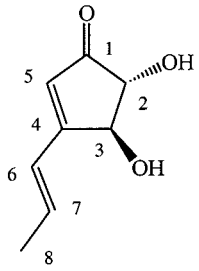

Figure 1. Structure of terrein, showing numbering used.

B3LYP[17] with the D95* basis set. Tensors for all structures were calculated using B3PW91[17a,18] and the D95** basis.

Fitting of the computed principal values versus H−O−C2−C1 and H−O−C3−C4 dihedral angles was performed using Maple 6.0. Surfaces were created using a least-squares fit to a Fourier series of the form $f(\alpha,\beta) = a + f(\alpha)f(\beta)$, where

$$f(\alpha) = \sum_{i=1}^{3}(b_i \cos(i\alpha) + c_i \sin(i\alpha))$$

$$\text{and } f(\beta) = \sum_{j=1}^{3}(b'_j \cos(j\beta) + c'_j \sin(j\beta))$$

The α and β denote the H−O−C2−C3 and H−O−C3−C4 dihedral angles, respectively, and the coefficients, *a*, *b*, *c*, ..., represent the least-squares adjustable parameters of the fit. The Fourier surfaces fit ab initio computed principal values with an RMS residual of ±1.2 ppm. An overall error was computed by subtracting a given experimental shift from all points in the corresponding surface, computing a squared difference and then summing these differences for all surfaces, and taking the square root of the resulting value. In terrein, a standard error of 1.68 ppm was found for the best-fit α and β orientations when principal values of only carbons 2 and 3 were considered. At each point in the composite 2D surface, an F-value was computed, and the *F*-value versus α and β angle was plotted to establish both stereochemistry and molecular conformation.

Thirty-nine and 31 conformations of terrein were initially selected at random for the 2*R*,3*S* and 2*S*,3*S* diastereomers, respectively, and corresponding tensor surfaces were computed. An additional 43 randomly selected points were subsequently computed for the best-fit 2*R*,3*S* isomer in the region of highest probability (α = 35−75° and β = 10−130°) using a grid divided into random 2° and 5° increments to improve the fit. Final conformational predictions were made from a Fourier fit to the region from 0 to 240° in both α and β and included 68 computed conformations for the 2*R*,3*S* isomer.

Results and Discussion

Terrein is a bioactive fungal metabolite (Figure 1) with two stereocenters and a relatively simple structure. Terrein can form only four stereoisomers and has limited conformational flexibility making it an ideal structure for an investigation of the relationship between relative stereochemistry and tensor shifts. Experimental ^{13}C tensor principal values for terrein were measured using the FIREMAT technique.[3a] FIREMAT resolves tensor patterns for individual nuclei by separating them into a second dimension by the differences in their isotropic shifts (see Figure 2). Before the relationship of tensor principal values to stereochemistry can be investigated, however, isotropic shifts must be correctly assigned to molecular positions.

In terrein, shift assignments were made by first separating the lines into subsets of different carbon types (i.e., CH_3, CH_2, CH, or quaternary) based on solid-state spectral editing techniques.[19] A comparison of experimental principal values with

(10) Harper, J. K.; Arif, A. M.; Li, J. Y.; Strobel, G.; Grant, D. M. *Acta Crystallogr.* **2000**, *C56*, e570.
(11) Dixon, W. T. *J. Chem. Phys.* **1982**, *77*, 1800.
(12) Bennett, A. E.; Reinstra, C. M.; Auger, M.; Lakshmi, K. V.; Griffen, R. G. *J. Chem. Phys.* **1995**, *103*, 6951.
(13) Sethi, N. K.; Alderman, D. W.; Grant, D. M. *Mol. Phys.* **1990**, *71*, 217.
(14) Ditchfield, R. *Mol. Phys.* **1974**, *27*, 789.
(15) Frisch, M. J.; Trucks, G. W.; Schlegel, H. B.; Scuseria, G. E.; Robb, M. A.; Cheeseman, J. R.; Zakrzewski, V. G.; Montgomery, J. A. Jr.; Stratmann, R. E.; Burant, J. C.; Dapprich, S.; Millam, J. M.; Daniels, A. D.; Kudin, K. N.; Strain, M. C.; Farkas, O.; Tomasi, J.; Barone, V.; Cossi, M.; Cammi, R.; Mennucci, B.; Pomelli, C.; Adamo, C.; Clifford, S.; Ochterski, J.; Peterson, G. A.; Ayala, P. Y.; Cui, Q.; Morokuma, K.; Malick, D. K.; Rabuck, A. D.; Raghavachari, K.; Foresman, J. B.; Cioslowski, J.; Ortiz, J. V.; Baboul, A. G.; Stefanov, B. B.; Liu, G.; Liashenko, A.; Piskorz, P.; Komaromi, I.; Gomperts, R.; Martin, R. L.; Fox, D. J.; Keith, T.; Al-Laham, M. A.; Peng, C. Y.; Nanayakkara, A.; Challacombe, M.; Gill, P. M. W.; Johnson, B.; Chen, W.; Wong, M. W.; Andres, J. L.; Gonzalez, C.; Head-Gordon, M.; Replogle, E. S.; Pople, J. A. *Gaussian 98*; Revision A.9; Gaussian, Inc.: Pittsburgh, PA, 1998.
(16) Harper, J. K.; McGeorge, G.; Grant, D. M. *Magn. Reson. Chem.* **1998**, *36*, S135.
(17) (a) Becke, A. D. *J. Chem. Phys.* **1993**, *98*, 5648. (b) Lee, C.; Yang, W.; Parr, R. G. *Phys. Rev. B* **1988**, *37*, 785.
(18) Perdew, J. P.; Wang, Y. *Phys. Rev. B* **1992**, *45*, 13244.

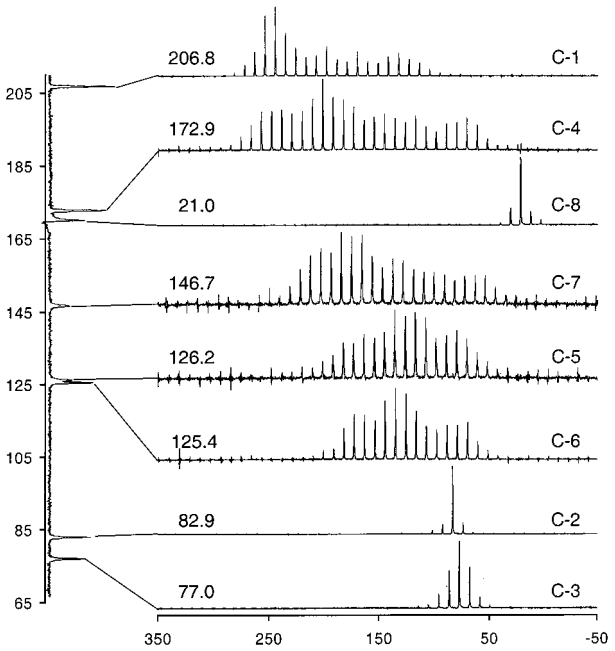

Figure 2. FIREMAT spectrum of terrein. Isotropic peaks are shown along the left side of the figure and corresponding tensors sideband patterns displayed horizontally. Assigned carbon numbers and corresponding isotropic shifts are listed on each sideband pattern. The isotropic peak displayed near 170 ppm (carbon 8) is aliased from its true position at 21.0 ppm for convenience in data collection.

Table 1. Principal Values of Terrein

carbon no.	chemical shift (ppm): experiment (theory[a])			
	δ_{11}	δ_{22}	δ_{33}	$\delta_{\text{Isotropic}}$[b]
1	268.1 (282.3)	250.9 (231.5)	101.4 (105.6)	206.8 (206.5)
2	96.0 (98.2)	79.8 (75.8)	72.8 (70.0)	82.9 (81.4)
3	98.2 (100.5)	77.3 (72.0)	55.4 (51.2)	77.0 (74.6)
4	277.7 (275.0)	197.8 (194.0)	43.1 (43.7)	172.9 (170.9)
5	206.8 (203.2)	123.8 (125.6)	48.0 (57.1)	126.2 (128.6)
6	191.8 (218.9)	133.9 (113.5)	50.7 (52.6)	125.4 (128.3)
7	232.7 (241.2)	175.2 (168.7)	32.3 (25.3)	146.7 (145.1)
8	31.7 (34.9)	24.5 (32.0)	6.7 (1.7)	21.0 (22.9)

[a] Theoretical principal values, given in parentheses, computed using the B3PW91 method and the D95** basis set. Structure used consisted of X-ray heavy atom positions with hydrogens (excluding hydroxy hydrogens) refined with the B3LYP method and the D95* basis set. Hydroxy hydrogens were fixed at X-ray-determined positions. [b] Isotropic shifts determined from a TOSS spectrum.

ab initio computed values was then used to make assignments within a subgroup. Specifically, within a subgroup of a given carbon type all possible arrangements of experiment with computed tensors were made, and the arrangement with the best fit was retained. An *F*-test established a probability of any given assignment relative to other possibilities. In terrein all shifts were assigned at better than 82% probability, and these assignments are given in Table 1.

To investigate the sensitivity of ^{13}C tensors to stereochemistry an approach is used in which computer-generated models of a variety of conformers are made for each diastereomer and tensors computed for energy-minimized structures. The best match of computed tensors to experimental values is accepted as the most probable structure. A statistical significance may be assigned to the proposed stereoisomer by comparing in an *F*-test the variance of the best match with experiment with the variance found for other possible structures. It is noted that use

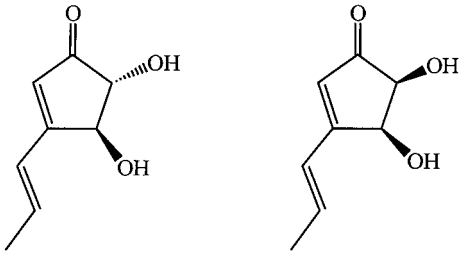

Figure 3. Structures of the 2*R*,3*S* and 2*S*,3*S* diastereomers examined. Tensor principal values cannot differentiate absolute stereochemistry; hence, a comparison of 2*R*,3*S* and 2*R*,3*R* or 2*S*,3*R* and 2*R*,3*R* or 2*S*,3*R* and 2*S*,3*S* are equivalent to the diastereomeric pair shown.

Table 2. Conformations of the 2*R*,3*S* and 2*S*,3*S* Diastereomers (Denoted by 1 and 2, respectively) Selected for Analysis[a]

H−O−C3−C2 dihedral angle \ H−O−C2−C1 dihedral angle	0	30	60	90	120	150	180	210	240	270	300	330	360
0		2							2	1			
30		1, 2	1	2	2	1, 2		1				2	
60				1			1	1			1		
90	2	1	1	1	1					2		1	2
120	2	1, 2	2	1		1	2				1		2
150		2	2	2					1		2	1	
180					1	1		1		1	1	1	
210				2		2							
240		1	1, 2		2	1		1, 2			1	1	
270		1			2	1					1		
300		2	2	2	2	2	1			1	1		
330												1, 2	
360													

[a] Shaded cells denote sterically unlikely orientations of the two hydroxy hydrogens relative to one another in the 2*S*,3*S* stereoisomer. No such steric restrictions on dihedral angle were found for the 2*R*,3*S* diastereomer.

of only tensor principal values potentially allows for the differentiation of diastereomers but not enantiomers. Hence, only relative stereochemistry may be established by this technique. In terrein we investigate the possibility of differentiating the 2*R*,3*S* stereoisomer from the 2*S*,3*S* diastereomer (Figure 3). However, an investigation of any other diastereomeric pair (i.e. 2*R*,3*S* vs 2*R*,3*R*, 2*S*,3*R* vs 2*R*,3*R* or 2*S*,3*R* vs 2*S*,3*S*) is equivalent, and only one pair is considered here for clarity.

Better selectivity of both stereochemistry and conformation is achieved when this comparison is performed using only principal values from the stereocenters (C2 and C3 in this case). Fortunately, remote structural features, known to influence shifts,[20] also confirm the stereochemistry but with less sensitivity. The X-ray structure of terrein has recently been described, allowing independent confirmation of all stereochemical conclusions obtained here from NMR.[10]

The proposed NMR approach presumes the availability of accurate tensor computation methods. Fortunately, previous computations on related natural products have shown that the errors in computed tensors are relatively small (2.1 and 3.3 ppm for sp^3 and sp^2 carbons, respectively) and reproducible.[2c,16] For typical molecules of this series these errors represent 3−15% and 1−2% of the tensor span (i.e., $\delta_{11}-\delta_{33}$) for sp^3 and sp^2 carbons, respectively.

Ideally, it would be desirable to investigate the sensitivity of ^{13}C tensors to stereochemistry independent of other factors. However, many structures exhibit significant conformational diversity that must also be included in the stereochemical analysis. While terrein is quite rigid, the hydroxy hydrogens at carbons 2 and 3 have considerable conformational freedom and potentially may assume a variety of orientations. In crystalline lattices, these H−O−C−C dihedral angles are usually dictated

(19) Hu, J. Z.; Harper, J. K.; Taylor, C.; Pugmire, R. J.; Grant, D. M. *J. Magn. Reson.* **2000**, *142*, 326.

(20) Pihlaja, K.; Kleinpeter, E. *Carbon-13 NMR chemical shifts in structural and stereochemical analysis*; VCH: New York, 1994; Chapter 3.

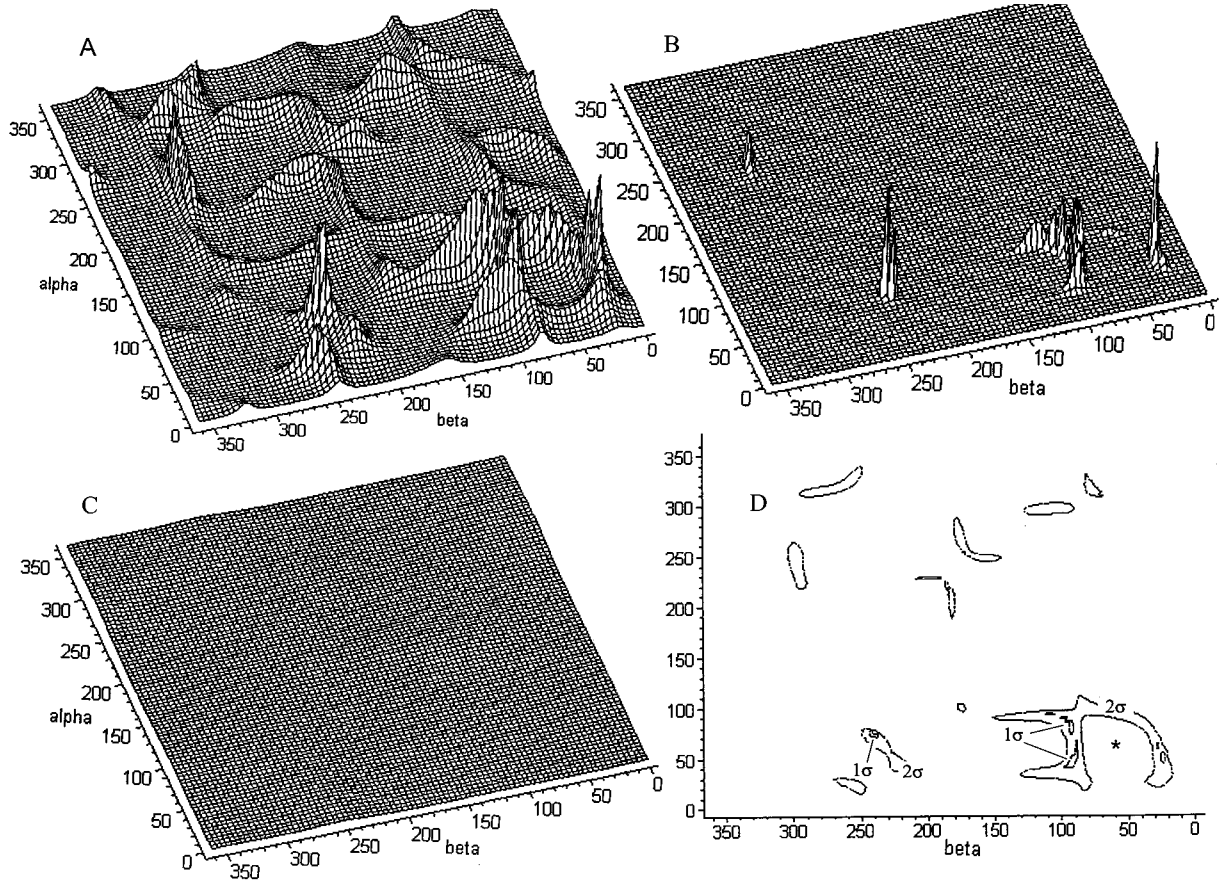

Figure 4. Probability surfaces illustrating the superior fit of the 2*R*,3*S* stereoisomer (A) to the experimental data. In contrast, the 2*S*,3*S* diastereomer (C) is a poor fit to experiment, regardless of conformation chosen. The 2*R*,3*S* diastereomer can be differentiated from the best matched 2*S*,3*S* diastereomer with a high statistical probability of >99.5%. Plot B shows an alternative processing of the data in A, the *Z*-surface, which provides more visually distinguishable local maxima. The contour plot D lends statistical meaning to plots A and B by showing the 1 and 2 standard deviation contour levels (68.3 and 95.5% probability levels, respectively). Unlabeled contours in D indicate the 2σ level. The X-ray-determined angles are indicated by an asterisk. The surface shown is under sampled and only allows selection of approximate areas for further investigation. The vertical scales in plots A and C are identical and represent the inverse *F*-value. The α and β angles denote the H−O−C2−C1 and H−O−C3−C2 angles, respectively.

by hydrogen bonding, both of the intra- and intermolecular type, making optimization of these angles in isolated molecules irrelevant. Where no lattice information is available, creating multiple conformationally varied models for each diastereomer accommodates this flexibility. To avoid the considerable computational cost involved in computing all possible conformations, a variety of H−O−C2−C1 and H−O−C3−C2 angles (α and β, respectively) are selected with a Monte Carlo sampling scheme. Approximately 20% of α and β orientations were sampled on a grid constructed with the full range of angles divided into 30° increments. The random sampling scheme selected 30−40 points for both the 2*R*,3*S* and 2*S*,3*S* isomers. The selected points were then examined for unfavorable O−H···H steric interactions between proximate atoms. The shaded regions of Table 2 show sterically unfavorable conformations found and result in the elimination of one conformation of the 2*S*,3*S* stereoisomer. A Fourier series fit of the 2D surface of inverse *F*-values versus α and β identify the regions of best fit. Additional randomly selected samples were then computed around local maxima ($\alpha = 45°$, $\beta = 25°$ and $\alpha = 70°$, $\beta = 90°$) of the 2*R*,3*S* stereoisomer using a grid divided into 2° and 5° increments. This second surface, fit to the sub-region, identifies the global maximum in the two-dimensional array. This Monte Carlo approach has the advantage of simultaneously establishing both relative stereochemistry and molecular conformation at a reduced computational cost.

The principal shift values of carbons 2 and 3 in terrein clearly identify the 2*R*,3*S* stereoisomer as the most probable (>99.5% probability level) from a comparison of theoretical and experimental results shown in Figure 4, A and C. This conclusion corresponds with the X-ray analysis.[10] Figure 4B presents an alternative data processing of plot A. This *Z*-surface[21] in plot B provides more visually distinguishable local maxima as it exponentially suppresses marginally less probable conformations. Plot D characterizes high probability regions of molecular conformations that are appropriate for both plots A and B. The 1 and 2 standard deviation levels are depicted in plot D along with X-ray-determined angles indicated by an asterisk. Inclusion of additional data points sampled near the local maxima in plots A and B provide a domain of high probability for α and β hydroxy dihedral angles (Figure 5). The X-ray-determined conformations of $\alpha = 68°$ and $\beta = 60°$ are contained within the area selected by NMR, validating the approach chosen.

Aside from inaccuracies introduced by the data analysis, the relatively large range in the NMR-determined angles might reflect a number of different factors that would be premature to address in this study. Among these are: (i) the neglect of electrostatic lattice-fields in the chemical shift calculations. Significant improvement in computed tensors has been dem-

(21) Le, H.; Pearson, J. G.; de Dios, A. C.; Oldfield, E. *J. Am. Chem. Soc.* **1995**, *117*, 3800.

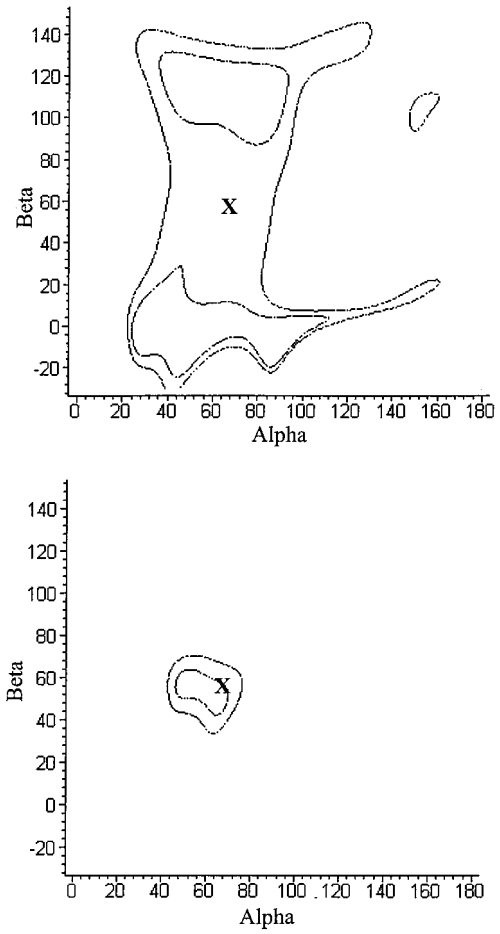

Figure 5. Contour maps showing selection of high probability dihedral angles for α and β in terrein when additional data points near the local maxima (α = 35−70°, β = 10−130°) are included for the 2*R*,3*S* diastereomer. The top plot ignores motional disorder and displays contours at the 90 and 80% probability levels. In the lower plot, the effect of conformational disorder in α and β is shown. Conformational averaging of α and β by ±20° and ±60°, respectively, about any given point was performed. The lower figure includes contours at one standard deviation and the 80% probability levels. The angle, α, is defined such that 0° denotes the O−H eclipsing the C1−C2 bond, and subsequent increases in angle indicate rotation toward the C2−H bond. The β angle is likewise defined with 0° as the angle with the O−H eclipsing the C2−C3 bond, and positive increments of angle denote rotation toward the C3−C4 bond. The X-ray-determined conformation is indicated with an X.

onstrated in cases where formal charges or highly polar molecules are encountered.[22] (ii) The broad range in NMR-determined angles alternatively might reflect considerable conformational disorder in the hydroxy hydrogens. Such hydrogen-bond disorder is known to occur and involves hydroxy protons switching between different hydrogen-bonded oxygens.[23]

Conformational disorder can be modeled by convoluting two or more theoretical models. Averaging of theoretical shifts for β angles separated by 120° will mix two regions of high probability in the β angle separated by ±60°. Two librating α angles separated by 40° produce a corresponding averaging of ±20°. In Figure 5, the top plot without averaging is widely dispersed. The convoluted model offers a much tighter fit of the NMR data, as shown in the lower plot of Figure 5, and produces an average conformation in good agreement with the X-ray value. The best-fit of NMR dihedral angles are found at $\alpha_{ave} = 52° \pm 12°$ and $\beta_{ave} = 58° \pm 11°$. These average values compare well with the corresponding X-ray values of $\alpha = 68°$ and $\beta = 60°$, portending promise for future NMR work on compounds in which X-ray data may be unavailable. Additional investigation hopefully will clarify the relative importance of the proposed origins of diversity in the NMR data.

Table 3. Maximum Differences in Computed Shifts for the Sampled Conformations of the 2*R*,3*S* and 2*S*,3*S* Diastereomers of Terrein

carbon no.	2*R*,3*S*			2*S*,3*S*		
	$\Delta\delta_{11}$	$\Delta\delta_{22}$	$\Delta\delta_{33}$	$\Delta\delta_{11}$	$\Delta\delta_{22}$	$\Delta\delta_{33}$
1	7.1	24.6	9.7	8.9	24.6	6.3
2	22.5	11.1	8.2	27.4	21.4	24.0
3	15.7	14.0	9.5	21.1	11.5	6.1
4	7.9	18.8	5.5	11.9	22.9	10.5
5	16.5	5.0	4.9	19.0	8.3	6.7
6	4.5	4.2	5.9	4.0	2.7	5.5
7	16.7	27.9	4.2	15.6	28.2	3.2
8	1.1	0.8	0.9	1.5	1.6	0.9

Variations in computed ^{13}C tensors arise from both stereochemical and conformational factors, creating changes that are significantly larger than found in either feature alone. In terrein, changes in ^{13}C principal values as large as 27.9 ppm are observed for different conformations of the two hydroxy hydrogens in the 2*R*,3*S* isomer. The 2*S*,3*S* diastereomer has similar variations with changes as large as 28.2 ppm. In contrast, conformational changes involving a single hydroxy hydrogen typically cause variations of less than 12 ppm.[6a] However, separating the shift variations observed in terrein into contributions from either conformational or stereochemical factors is not straightforward because of the rather complicated interplay between the two structural features. Since errors in computed ^{13}C tensors remain roughly the same as in the uncoupled case, these larger variations have the overall effect of increasing the confidence in statistical characterization of both conformation and stereochemistry.

Carbons 2 and 3 strongly reflect changes in both stereochemistry and conformation. Significant changes are also found at C1 (δ_{11}, δ_{22}, and δ_{33}), C4 (δ_{11} and δ_{22}), C5 (δ_{11}), and C7 (δ_{11} and δ_{22}) as summarized in Table 3. Inclusion of these additional carbons also correctly identifies the stereochemistry, albeit at a decreased statistical significance (roughly 85% probability) because of reduced sensitivity of these positions to the local structure at C2 and C3. The large variations observed in these additional carbons appear to reflect other structural features unrelated to the structure at C2 and C3. Generally, it appears that inclusion of only those carbons directly involved in the structural variations offers the most accurate analysis.

Isotropic ^{13}C shifts potentially have the capacity of also providing the stereochemical and conformational information. Furthermore, they are usually easier to measure. A corresponding comparison was therefore made to determine the sensitivity of isotropic shifts. The computed isotropic values for carbons 2 and 3 select the correct 2*R*,3*S* stereochemistry as the best fit with roughly an 80% probability. However, α and β dihedral angles are much less sensitive to isotropic shifts with nearly 80% of the sampled points on the surface statistically indistinguishable from each other. Hence, carbon principal shift data offer a superior assessment of both stereochemistry and molecular conformation.

(22) (a) Stueber, D.; Guenneau, F. N.; Grant, D. M. *J. Chem. Phys.* **2001**, *114*, 9236. (b) de Dios, A. C.; Oldfield, E. *Chem. Phys. Lett.* **1993**, *205*, 108. (c) de Dios, A. C.; Laws, D. D.; Oldfield, E. *J. Am. Chem. Soc.* **1994**, *116*, 7784.

(23) Jeffery, G. A. *An Introduction to Hydrogen Bonding*; Oxford University Press: Oxford, UK, 1997; pp 117−119.

Conclusions

The comparison of solid-state NMR tensor data with ab initio computed tensors allows both relative stereochemistry and conformation in terrein to be established with relatively high statistical significance. In terrein, the stereochemistry of 2R*,3S* is obtained, consistent with X-ray conclusions. Variations in computed tensors for different conformations of a given diastereomer are roughly 10 times larger than the estimated error. This demonstrates that conformational variations in spatially close groups are strongly correlated with structure, providing a method for assigning structure with high statistical confidence. Extensions of the proposed methodology to molecules with greater conformational flexibility appear to be feasible on the basis of the results obtained for terrein and are currently being pursued.

Acknowledgment. Computer resources for tensor computations were provided by the Center for High Performance Computing at the University of Utah. This work was supported by the National Institute of Health under Grant GM 08521-39 to D.M.G., and funding from the Montana Agricultural Experiment Station and the National Science Foundation to G.S.

JA010997L